Separation Science and Technology
Publication details, including instructions for authors and subscription information:
http://www.informaworld.com/smpp/title~content=t713708471

The Influence of Chemical Reaction on Mass Transfer Behavior in the Membrane Absorption Process

Jian Gao[a]; Weidong Zhang[a]; Shu Chen[a]; Zeting Zhang[a]
[a] The Ministry of Education Key Laboratory of Science and Technology of Controllable Chemical Reactions, Beijing University of Chemical Technology, Beijing, PR China

To cite this Article Gao, Jian , Zhang, Weidong , Chen, Shu and Zhang, Zeting(2005) 'The Influence of Chemical Reaction on Mass Transfer Behavior in the Membrane Absorption Process', Separation Science and Technology, 40: 6, 1227 — 1244
To link to this Article: DOI: 10.1081/SS-200052833
URL: http://dx.doi.org/10.1081/SS-200052833

Separation Science and Technology, 40: 1227–1244, 2005

ISSN 0149-6395 print/1520-5754 online
DOI: 10.1081/SS-200052833

The Influence of Chemical Reaction on Mass Transfer Behavior in the Membrane Absorption Process

Jian Gao, Weidong Zhang, Shu Chen, and Zeting Zhang
The Ministry of Education Key Laboratory of Science and Technology of Controllable Chemical Reactions, Beijing University of Chemical Technology, Beijing, PR China

Abstract: Special reaction systems were proposed to investigate the mechanism of the mass transfer process in the membrane absorption process. The mass transfer resistance of this process was calculated by using hydrophobic polypropylene (PP) hollow fiber membrane (HFM); and a 2-order partial differential model, including reaction, was developed to describe the SO_2 and CO_2 absorption process using HFM. Throughout the experimental analyzing and model results, for either SO_2/air/NaOH system or CO_2/air-NaOH system, different phenomena in these two systems were discussed. Since the reaction mechanisms of both the SO_2-NaOH system and the CO_2-NaOH system were different, the SO_2 and CO_2 mass transfer in liquid side were different. The relation between the chemical reaction mechanism and mass transfer, instead of the ionized effect, was the reason for deviation in SO_2 absorption process. The influence of liquid phase velocity and the concentration of absorbent on the mass transfer process was also discussed.

Keywords: Membrane absorption, mass transfer resistance, boundary layer, mathematic simulation

Received 6 July 2004, Accepted 9 December 2004
Address correspondence to Weidong Zhang, College of Chemical Engineering, The Ministry of Education Key Laboratory of Science and Technology of Controllable Chemical Reactions, Beijing University of Chemical Technology, PO Box 1#, Beijing 100029, PR China. E-mail: zhangwd@mail.buct.edu.cn

INTRODUCTION

The use of the membrane absorption process, based on the membrane, is a potent technique in the field of removal of pollution gases like SO_2, CO_2, H_2S, CO, and NH_3, etc. The membrane absorption combines the advantages of both the membrane process and the absorption process. The gas phase and the liquid phase (absorbent) flow along the different sides of membrane, and contact each other through the micropores of the membrane (1). Compared to the traditional absorber, the membrane absorber can overcome the shortcoming of flooding, loading, channeling, and lower efficiency, etc.

Kreulent et al. (2) used different materials (nonwetted and wetted) of flat membranes in a stirred cell reactor to carry out the mass transfer experiments and concluded that nonwetted membranes were to be preferred for a fixed interface in gas/liquid absorbers with membranes. Hollow fiber membrane (HFM) was also studied in this process because the HFM can provide a larger contact area than can the conventional gas/liquid contact equipment. It was reported by Mastson et al. (3) that the specific contact area of HFM modules was about $8000\,m^2/m^3$. Qi and Cussler (4) developed the idea of the HFM module using a microporous hydrophobic polypropylene HFM to carry out mass transfer experiments and studied absorption of NH_3 in water, and H_2S and SO_2 in aqueous NaOH. They found, in all these cases, that the absorption process was predominately controlled by the diffusion across the membrane. Nii et al. (5) published a study on the absorption of CO_2 in ammoniacal cuprous chloride solutions using HFM absorbers that can be more efficient than conventional absorbers. Kim and Seung-Man Yang (6) studied the CO_2 absorption rate using aqueous solutions of amines with PTFE-HFM absorber in the temperature range from 20 to 60°C. It was found that as temperature rises, the absorption rate of CO_2 increases.

In a previous study, a resistance-in-series model was established to describe the mass transfer process. However, few theoretical analyses were performed to describe the HFM absorber (7–9). Calabrò (10) studied the mass transfer behavior of hollow fiber membrane bioreaction. It constituted a second-order mass transfer model including the reaction. The concentration profile of reacting mass and production were calculated by numerical solution. However, the influence of different reaction mechanisms was not analyzed. Lee et al. (11) analyzed mass transfer behavior of CO_2 using an HFM in which K_2CO_3 solution flows as an absorbent flowing in lumen. They also considered reaction and used a numerical solution to solve a second-order mass transfer model. But similar to Calabrò, they investigated only one system. In the model of that study, there were comparisons between the two systems and analyses of the profile of all components on the liquid side. The different reaction mechanism will seriously affect the mass transfer process. In the

experiment involving SO_2-NaOH membrane absorption process, there was deviation between experimental data and predicted value. Similar phenomena were also found in the experiment of Qi and Cluesser (4), and they explained it was due to the influence of ionization. But the hypothesis of ionization cannot explain the results in other experimental systems, which had the same ionized effect and similar reaction steps as the CO_2-NaOH system that had no deviation between experimental data and predicted value (2–6). Therefore, further study of acid gas membrane absorption with chemical reaction was necessary.

In this work, two reaction systems (SO_2/air–NaOH and CO_2/air–NaOH) were proposed to investigate the different mass transfer behavior of SO_2 and CO_2 in solution, which had similar ionization effects. In addition, the experimental results were compared with a second-order partial differential model including a reaction that was developed to describe the SO_2 and CO_2 absorption process with HFM.

THEORY

Resistance-in-Serials Model

Recently, many researchers have used a *resistance-in-serials model* to describe the membrane absorption process. For hydrophobic membranes, the overall mass transfer coefficient based on gas phase was given as the model:

$$\frac{1}{K_G} = \frac{1}{k_G} + \frac{1}{k_m} + \frac{1}{m\beta k_L} \tag{1}$$

Where, the three individual mass transfer coefficient, k_G, k_m, and k_L, can be calculated by the individual empirical correlations. For this experimental system the gas was sent at the tube side and the liquid was fed at the shell side, the following correlations were chosen according our calculation (12, 13).

$$k_L = 5.9 \cdot \frac{D_L}{d_e} \cdot \left(\frac{d_e^2 u_L}{l\nu}\right)^{2/3} \left(\frac{\nu}{D_L}\right)^{1/3} \tag{2}$$

$$k_G = 1.62 D_{AG} d_i^{-2/3} \left(\frac{R_e S_c}{l}\right)^{1/3} \tag{3}$$

$$k_m = D_M \frac{\varepsilon}{\delta\tau} \tag{4}$$

Numerical Model

In order to investigate the detail of the mass transfer behavior in the gas HFM absorption process with a chemical reaction, the profile of the mass transfer component on the liquid side should be obtained, and then it can be used to describe the influence of a chemical reaction on the mass transfer in the HFM absorption process with chemical reaction.

In this study, the class reaction–diffusion equation was used to describe the reactive absorption process of a gas in a liquid flowing through a microporous hollow fiber based on the following assumptions: 1) select a single hollow fiber as the object of simulation; 2) compared to the shell-side diameter, the fiber diameter can be ignored; 3) steady state; 4) axial symmetry; 5) axial diffusion and radial flux were ignored. Radial diffusion keeps to Fick's law; 6) ideal gas behavior and complying with Henry's law. The coordinate and mass balances differential of the HFM absorber in this experiment are shown in Fig. 1. The coordinates of r and z were shown for the numerical analysis. The I_r and I_z were, respectively, the mass input to the differential mass balances cell of radial and axial direction, and the Q_r and Q_z were respectively the mass output to the differential mass balances cell of radial and axial direction. The differential mass balance for the component, i, present in the liquid side was given by

$$u_z \frac{\partial C_i}{\partial z} = D_i \left[\frac{\partial^2 C_i}{\partial r^2} + \frac{1}{r} \frac{\partial C_i}{\partial r} \right] + R_i \tag{5}$$

According to the assumption, Eq. (3), the u_z was constant.

$$A + B \underset{k_{-1}}{\overset{k_1}{\rightleftharpoons}} E \tag{6}$$

$$E + B \underset{k_{-2}}{\overset{k_2}{\rightleftharpoons}} F + H_2O \tag{7}$$

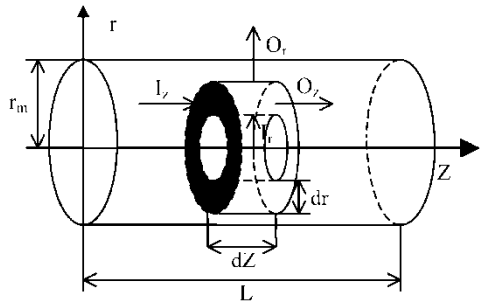

Figure 1. Schematic coordinates of the HFM absorber and its differential mass balances cell.

For the 2-set-ups reaction, the form was the same as that in Eqs. (6) and (7), between the gas and liquid phase, the reaction rates of all components were given by

$$R_A = k_{-1}C_E - k_1 C_A C_B \tag{8a}$$

$$R_B = k_{-1}C_E - k_1 C_A C_B + k_{-2}C_F - k_2 C_E C_B \tag{8b}$$

$$R_E = k_1 C_A C_B - k_{-1}C_E + k_2 C_E C_B - k_{-2}C_F \tag{8c}$$

$$R_F = k_2 C_E C_B - k_{-2}C_F \tag{8d}$$

Where k_1 and k_{-1} were, respectively, the forward and reverse rate constant of Eq. (6), and k_2 and k_{-2} were, respectively, the forward and reverse rate constant of Eq. (7). In these equations, the "A" was used to denote SO_2 or CO_2, the "B" to denote the hydroxyl ion (OH^-), the "E" to denote the univalent ion (HSO_3^- or HCO_3^-), and the "F" to denote the bivalent ion (SO_3^{2-} or CO_3^{2-}).

Substituting Eq. (8) to Eq. (5), transforms into the dimensionless equations Equation (9) can be modified for A, B, E, and F, respectively.

$$\frac{\partial C'_A}{\partial Z} = D_{cA}\left[\frac{\partial^2 C'_A}{\partial r'^2} + \frac{1}{r'}\frac{\partial C'_A}{\partial r'}\right] + \frac{k_{-1}C_{E0}C'_E - k_1 C_{A0}C_{B0}C'_A C'_B}{C_{SA}} \tag{9a}$$

$$\frac{\partial C'_B}{\partial Z} = D_{CB}\left[\frac{\partial^2 C'_B}{\partial r'^2} + \frac{1}{r'}\frac{\partial C'_B}{\partial r'}\right] + \frac{k_{-1}C_{E0}C'_E - k_1 C_{A0}C_{B0}C'_A C'_B + k_{-2}C_{F0}C'_F - k_2 C_{E0}C_{B0}C'_E C'_B}{C_{SB}} \tag{9b}$$

$$\frac{\partial C'_E}{\partial Z} = D_{CE}\left[\frac{\partial^2 C'_E}{\partial r'^2} + \frac{1}{r'}\frac{\partial C'_E}{\partial r'}\right] + \frac{k_1 C_{A0}C_{B0}C'_A C'_B - k_{-1}C_{E0}C'_E + k_{-2}C_{F0}C'_F - k_2 C_{E0}C_{B0}C'_E C'_B}{C_{SE}} \tag{9c}$$

$$\frac{\partial C'_F}{\partial Z} = D_{CF}\left[\frac{\partial^2 C'_F}{\partial r'^2} + \frac{1}{r'}\frac{\partial C'_F}{\partial r'}\right] + \frac{k_2 C_{E0}C_{B0}C'_E C'_B - k_{-2}C_{F0}C'_F}{C_{SF}} \tag{9d}$$

Where the dimensionless variables and dimensionless coordinates were defined as follows:

$$Z = \frac{z}{L},\ r' = \frac{r}{r_m},\ C'_i = \frac{C_i}{C_{i0}} \quad \text{and} \quad C_{Si} = \frac{u_z \cdot C_{i0}}{L}\ (i = \text{A, B, E, F}) \tag{10a}$$

Also the dimensionless parameters "diffusion rate" were defined as:

$$D_{ci} = \frac{L \cdot D_i}{u_z \cdot r_m^2} \ (i = \text{A, B, E, F}) \tag{10b}$$

The following initial and boundary conditions were subjected to:

$$\text{For all } r',\ Z = 0,\ C_i' = 1; \tag{11a}$$

$$\text{For all } Z,\ r' = 0, C_A' = 1 \text{ and } \frac{\partial C_B'}{\partial r'} = \frac{\partial C_E'}{\partial r'} = \frac{\partial C_F'}{\partial r'} = 0 \tag{11b}$$

$$\text{When } r' = 1,\ \frac{\partial C_A'}{\partial r'} = \frac{\partial C_B'}{\partial r'} \frac{\partial C_E'}{\partial r'} = \frac{\partial C_F'}{\partial r'} = 0 \tag{11c}$$

The radial position of $r' = 0$ denotes the center of the shell, and also the outside of the hollow fiber [assumption (2)], while $r' = 1$ represents the liquid boundary layer thickness.

The initial conditions for the absorption process were given in Eq. (11a). Because supposing inlet concentration as the denominator of dimensionless concentration ($C_i' = C_i/C_{i0}$), apparently $C_i' = 1$ at the inlet. In fact, A, E, and F were very small at the inlet of the shell side, but as a relative amount, it had no effect on the variation trend. In order to simplify the model, there was an hypothesis that the concentration of the component, A, didn't vary along the tube side of the fiber, so for all Z and $r' = 0$, the $C_A' = 1$.

The set of Eqs. (9) is a group of complex nonlinear partial differential equations and the orthogonal collocation method was used to solve them (9). This method was first put forward by Lanczos (14), for details of the solving process see the references (15, 16).

EXPERIMENTAL

The geometric characteristic of the HFM module used in this study is listed in Table 1. The membrane material used was polypropylene.

The mixture of SO_2 or CO_2 and air flow through the tube side of hollow fiber membrane, while the absorbent currently flows through the shell side of module counter. Since the membrane was hydrophobic, the micropores of membrane were filled by gas, the gas-liquid interface was on the outer side of hollow fiber membrane. The experimental apparatus used is shown in Fig. 2. The velocity of the gas phase was in the range of 0.08∼0.40 m/s, the velocity of absorbent was in the range of 0.012∼0.03 m/s, both the gas and liquid phases were laminar flow. Pure water and sodium hydroxide solution was used as the absorbent. The inlet concentration of SO_2 or CO_2 in the mixture was $(1.23\sim4.10) \times 10^{-4}$ mol/L (atmospheric pressure, 20°C), the concentrations of absorbent were 0 (pure water), 0.1, 0.8, and 1.0 mol/L, respectively.

Table 1. Structural parameter of PP HFM module

Shell i.d. (m)	1.6×10^{-2}
Number of fibers	500
Fiber i.d. (m)	3.4×10^{-4}
Membrane thickness (m)	4.3×10^{-5}
Average pore dia. (m)	3.0×10^{-8}
Membrane porosity (%)	0.51
Module Eff. length (m)	0.26

The experimental overall mass transfer coefficient can be calculated from Eq. (12):

$$K_{\mathrm{G}} = \frac{V_G}{A(1 - V_G/m \cdot V_L)} \ln \frac{C_{\mathrm{G1}} - C^*_{\mathrm{G1}}}{C_{\mathrm{G2}} - C^*_{\mathrm{G2}}}. \tag{12}$$

Since fresh absorbent was used, $C^*_{\mathrm{G2}} = 0$. In the condition when NaOH solution acts as absorbent, the concentration of SO_2 or CO_2 in liquid phase can be treated as 0, $C^*_{\mathrm{G1}} \approx 0$.

RESULTS AND DISCUSSION

The Different Mass Transfer Behavior Between the SO_2 and CO_2 HFM Absorption Processes

According to Eq. (1) and (2), when the gas velocity and other operating states didn't vary, the overall mass transfer resistance should be linearly to

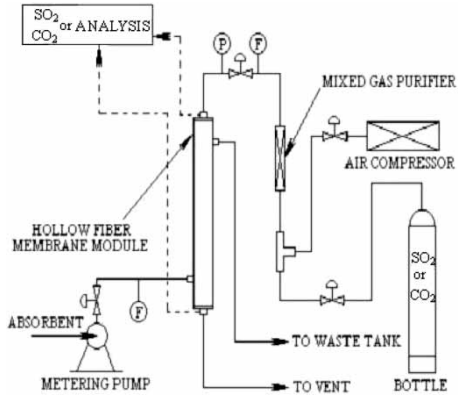

Figure 2. Experimental apparatus schematic diagram.

the minus two-thirds power of liquid velocity. However, the results from Fig. 3, show that there was deviation from the predicted value, and this deviation became serious when the concentration of NaOH in the absorbent was low.

A similar phenomenon was found in Qi and Cussler's report by using the same system (4). It was considered as the influence of ionization in the process of SO_2 absorbing to the liquid phase because the pK_a of SO_2 was 1.90. That means, in the aqueous phase, 66% of the absorbed SO_2 was ionized, and in the NaOH solution, the SO_2 being ionized was greater, thus the diffusion of SO_2 in the feed includes parallel transport of molecular SO_2, of HSO_3^-, and of SO_3^{2-}. So, there was deviation between the experimental result and the *resistance-in-serials* theory in the SO_2 HFM absorption process. However, this hypothesis cannot explain the result of the CO_2-NaOH system. The effect of ionization in the process of absorbing to NaOH solution was similar for these two systems, but that kind of deviation was not reported in the experiment of the CO_2-NaOH system (Fig. 4). There were other reasons that are discussed in detail in the section that follow.

The Simulation

In order to explain the different mass transfer behavior in the absorption process with chemical reaction, the form was similar to Eq. (6) and Eq. (7), the profiles of the component "B," "E," and "F" at radial and axial direction in the liquid boundary layer were calculated by the model [Eq. (9)] in order to investigate the influence between the molecular and ion mass transfer in this acid-gas HFM absorption process. The cause of investigation was that the concentration of the component "A" at inlet was higher or lower than was the concentration of the component "B" at inlet. The simulation results

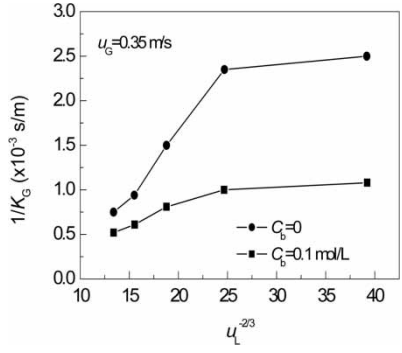

Figure 3. Effect of liquid velocity on overall mass transfer resistance when absorbing SO_2.

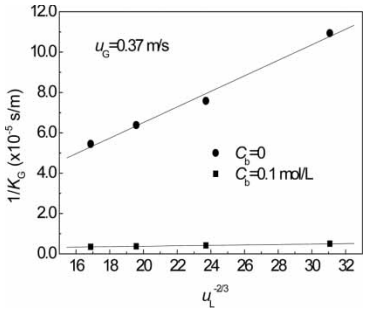

Figure 4. Effect of liquid velocity on overall mass transfer resistance when absorbing CO_2.

were discussed as follows. The parameters used in this model were obtained by the SO_2-NaOH and CO_2-NaOH system because these two systems were used in this experimental research, and the values of the parameters were shown in Table 2, respectively.

According to the references (17, 18), in general, the rate constant of the fast reaction was $>1.0 \times 10^5\,dm^3\,mol^{-1}\,s^{-1}$ and the slow one was $<1.0 \times 10^3\,dm^3\,mol^{-1}\,s^{-1}$ for the second-order reaction between the gas and liquid phase [the reaction form was similar Eqs. (6) and (7)]. In this simulation, it was not necessary for us to know the accurate absolute value of the rate constant of the reaction. It was, however, necessary for us to know the relative value of the rate constant of the reaction between the first step and second steps. At the same time, defining the chemical reaction showed that the first step was much faster than was the second step just like in the SO_2-NaOH system in the first case reaction and the reaction that the first step was much slower than was the second step was just like the CO_2-NaOH system in the second.

For the First Case Reaction

For the first case, Fig. 5 shows the dimensionless concentration of component E as a function of dimensionless radial distance with various axial dimensionless positions in the liquid boundary layer on condition that the concentration of the components A and B at inlet were 0.001 mol/m^3 and $1 \times 10^{-7}\,mol/m^3$,

Table 2a. Operating conditions for numerical analysis

u_Z ($m\,s^{-1}$)	C_A ($mol\,m^{-3}$)	C_B ($mol\,m^{-3}$)
0.02	0.001	1×10^{-7} or 0.001

Table 2b. Parameters of reaction rates and equilibrium

First	k_1 ($dm^3\,mol^{-1}\,s^{-1}$)	k_2 ($dm^3\,mol^{-1}\,s^{-1}$)	K_1 ($dm^3\,mol^{-1}$)	K_2 ($dm^3\,mol^{-1}$)
For the first case	1.0×10^3	1.0×10^5	6.53×10^{7a}	6.59×10^{3a}
For the second case	1.0×10^5	1.0×10^3	2.21×10^{12b}	9.86×10^{6b}

[a]It was calculated by according to the reference (19).
[b]It was calculated by according to the reference (20).

respectively. From Fig. 5, the numerical results clearly show that the concentration of component E increases as the radial distance increases and the concentration of component E was the highest at the liquid boundary layer. That is to say, there was accumulation of the component E in the liquid boundary for the HFM absorption process. In Fig. 6, the profile of the dimensionless concentration of component B at the radial direction with various axial dimensionless positions as shown. It was found that the supplement of component B in the liquid boundary layer was seriously short.

Figure 7 shows the profile of the dimensionless concentration of component F at the radial direction. One can find that the concentration of component F in the liquid boundary layer was much lower than was the concentration of the component E in the liquid boundary layer. That means, the second step reaction didn't occur smoothly for the first case because the second step reaction rate in the first case was low.

However, when the concentration of component B at the inlet increases (in this case, the concentrations of components A and B at the inlet were $0.001\,mol/m^2$ and $1\,mol/m^2$, respectively), there was no accumulation of component E in the liquid boundary (Fig. 8) because B was enough to consume the generation E ion in the liquid boundary in this case.

Table 2c. Diffusion coefficient of the component "*i*" in water (20°C) (21, 22)

	Component	Diffusion coefficient in water, D ($m^2 \cdot s^{-1}$)
For the first case	A	1.70×10^{-9}
	E	1.47×10^{-9}
	F	1.33×10^{-9}
For the second case	A	1.71×10^{-9}
	E	1.59×10^{-9}
	F	1.23×10^{-9}
	B	9.3×10^{-9}

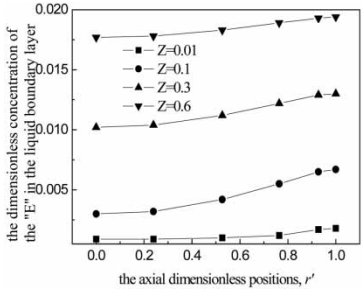

Figure 5. In the 1st case, the profile of the dimensionless concentration of the component "E" at the radial direction with various axial dimensionless positions, when the component "B" was short.

For the Second Case Reaction

For the second case, whether the concentration of component B at inlet was high or low, there was no accumulation of component E in the liquid boundary (Fig. 9) because of the reaction mechanism of the second case reaction system. In Fig. 9, one can find that the dimensionless concentration of component E in the liquid boundary layer didn't vary with the dimensionless radial distance when the axial dimensionless position was fixed.

The Theory Analyzing the Deviation of Mass Transfer Behavior in the SO_2 HFM Absorption Process

From the model analyzed earlier, the mass transfer behavior of the gas-HFM absorption process with a two-step chemical reaction whose reaction rate between each step was different, will be analyzed as follows.

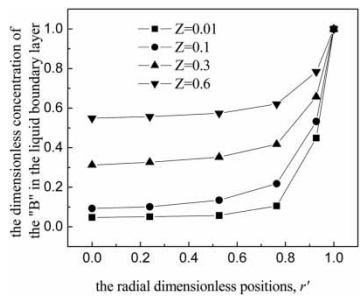

Figure 6. In the 1st case, the profile of the dimensionless concentration of the component "B" at the radial direction with various axial dimensionless positions when the "B" was short.

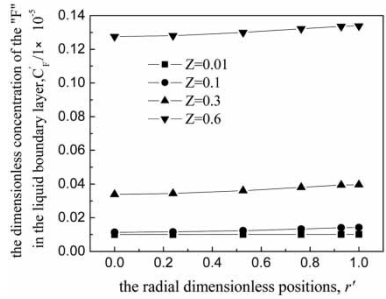

Figure 7. In the 1st case, the profile of the dimensionless concentration of the "F" at the radial direction with various axial dimensionless positions, when the "B" was short.

In the SO_2-HFM absorption process, when the concentration of NaOH was low, then the quantity of OH^- ion was also low; the generation of HSO_3^- ion can not be consumed instantly, which increases the accumulation of the HSO_3^- ion in the liquid boundary because of the reaction mechanism of the SO_2-NaON system.

The reaction of SO_2 absorbing to the NaOH solution has two steps:

$$SO_2 + OH^- \rightleftharpoons HSO_3^- \tag{13}$$

$$HSO_3^- + OH^- \rightleftharpoons H_2O + SO_3^{2-} \tag{14}$$

Since the first step reaction is very quick, while the second step is slower, in the gas/liquid interface of the absorbing process, there was an accumulation of HSO_3^- due to the excess of SO_2, the concentration of OH^- ion was not enough to neutralize the absorbed SO_2. According to the reaction shown in

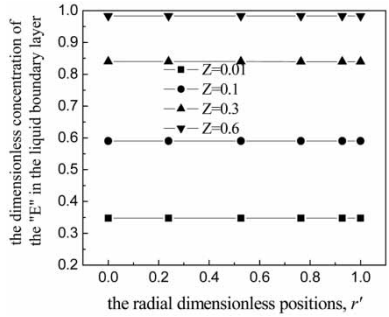

Figure 8. In the 1st case, the profile of the dimensionless concentration of the "E" at the radial direction with various axial dimensionless positions, when the "B" was enough.

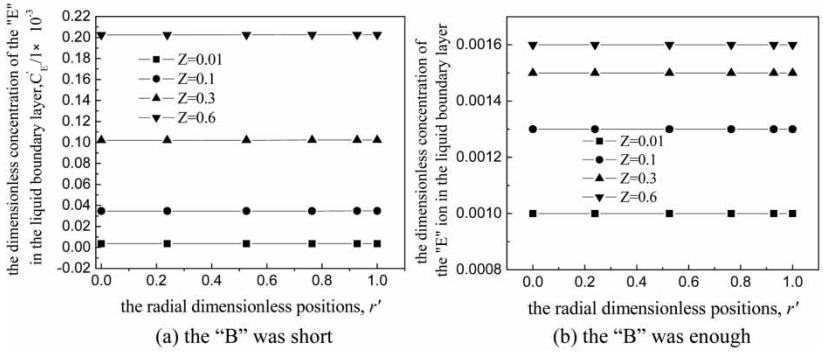

Figure 9. In the 2nd case, the profile of the dimensionless concentration of the "E" at the radial direction with various axial dimensionless positions.

Eq. (13), when the equilibrium constant for the reaction Eq. (13) was K, the concentration of SO_2 in the boundary layer of liquid phase can be written as:

$$[SO_2] = \frac{1}{K} \cdot \frac{[HSO_3^-]}{[OH^-]} \tag{15}$$

From Eq. (15), it can be found that when the concentration of NaOH in absorbent was low, due to the accumulation of HSO_3^-, the concentration of SO_2 in the boundary layer of the liquid phase would increase, and the mass transfer drive was reduced. With the increase of liquid velocity, the thickness of the mass transfers boundary layer will decrease. When the rate of gas/liquid velocity increase, the concentration of OH^- ion that enters into the liquid boundary layer is enough to react with the absorbed SO_2, so, the concentration of SO_2 in the boundary layer can be reduced, and the mass transfer drive increased. So from Fig. 3, we see the liquid velocity increase the relation between the overall mass transfer coefficient and the minus two-thirds the power of the liquid velocity level-off to linearity.

On the other hand, with increasing absorbent concentration, the concentration of OH^- ion increases, the enhance factor β, which was caused by chemical reaction enlarges. When β was large enough, according to the *Resistance-in-serials* theory, the contribution of liquid phase mass transfer resistance would be very small. So, the influence of chemical reaction to the overall mass transfer coefficient can be decreased, this interpretation agrees with the result shown in Fig. 10, the deviation with the *Resistance-in-serials model* was small compared to Fig. 3. At that time, the mass transfer process of the the SO_2-NaOH system was similar to the CO_2-NaOH system (Figs. 10 and 11).

The influence of the reaction mechanism on the HFM absorbing CO_2 process was smaller compared to the HFM absorbing SO_2 process because

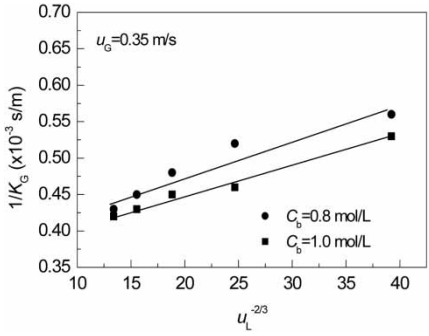

Figure 10. Effect of liquid velocity on overall mass transfer resistance when high concentration absorbent was used for SO_2 system.

of the different reaction mechanism of the SO_2-NaOH system. For the CO_2-NaOH system, the reaction also included two steps and follows as:

$$CO_2 + OH^- \rightleftharpoons HCO_3^- \tag{16}$$

$$HCO_3^- + OH^- \rightleftharpoons H_2O + CO_3^{2-} \tag{17}$$

For this system, since the second-step reaction is very quick while the first step is slow, in the gas/liquid interface of the absorbing process, there was little accumulation of HCO_3^- in the liquid boundary layer, and the result was that the HCO_3^- converts to CO_3^{2-} instantly, so the first step reaction [Eq. (16)] of this system was going on swimmingly for the whole absorption process. From analyzing the previous information, the mass transfer behavior of the CO_2 absorbing process agrees with the description in Eq. (16) and Eq. (17), which was in accord with the *Resistance-in-serials* model. That is

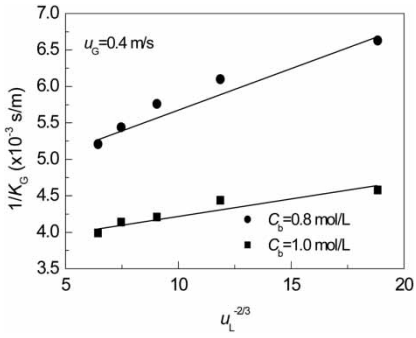

Figure 11. Effect of liquid velocity on overall mass transfer resistance when high concentration absorbent was used for CO_2 system.

to say, if the gas velocity remains fixed and the other operation conditions are the same, the overall mass transfer resistance should be linear to the minus two thirds power of liquid velocity, as was shown as Fig. 4 and Fig. 11.

Chemical Reaction Enhancement Effect for the SO_2 and CO_2 HFM Absorption Process

According to the previous analysis, the mechanisms of the chemical reaction enhancement effect for the SO_2 and CO_2 HFM absorption process were different. In the SO_2 HFM absorption process, the SO_2 mass transfer was baffled because of the reaction mechanism, which leads to accumulating the ion, HSO_3^-. But, when the concentration of the NaOH increases, not only the chemical enhancement factor, β, but also the concentration of the ion HSO_3^- in the liquid boundary layer, decreases because of the increasing concentration of the OH^- ion. However, in the CO_2 HFM absorption process, the reaction mechanism didn't affect the CO_2 mass transfer because of the mechanism of the CO_2-NaOH system and the increasing concentration of the OH^- ion only increases the chemical enhancement factor, β.

CONCLUSIONS

In this article, the SO_2/air-NaOH system and CO_2/air-NaOH system were similar two-step reactions, but their reaction mechanisms were different, respectively. We proposed to investigate the mass transfer behavior in the HFM absorption process. It was found that there was different mass transfer behavior between the SO_2 and CO_2 HFM absorption process. The reaction mechanism of the SO_2 and NaOH leads to the deviating from the *Resistance-in-serials* theory.

In order to do further research on the influence of the chemical reaction mechanism on this mass transfer process, a two-order model was developed to describe the behavior of mass transfer in the acid gas HFM absorption process with reaction. According to numerical results of the model, in the SO_2 HFM absorption process, when the concentration of NaOH at inlet was relatively low, there was accumulation of the HSO_3^- ion in the liquid boundary and the OH^- ion supplied in the liquid boundary was not enough because the first reaction step was much faster than the second reaction step in the reaction between the SO_2 and OH^- ion. When the concentration of NaOH at inlet increased, the accumulation of the HSO_3^- ion in the liquid boundary decreased because the OH^- ion supplied in the liquid boundary increased. However, for the CO_2 HFM absorption process, there was no accumulation of the HCO_3^- ion in the liquid boundary and the chemical reaction goes on smoothly because the first reaction step was much slower

than the second reaction step in the reaction between the CO_2 and OH^- ion. So, the mass behavior accords with the *resistance-in-serial*, theory whether the concentration of NaOH at inlet was high or low.

NOMENCLATURE

C_A, C_B, C_E, C_F	The concentration of the A, B, E, and F, respectively (mol/m^3)
C_A', C_B', C_E', C_F'	The dimensionless concentration of A, B, E, and F, respectively (−)
C_{A0}, C_{B0}, C_{E0}, C_{F0}	The initial concentration of A, B, E, and F, respectively (mol/m^3)
$C\text{-}_{SA}$, C_{SB}, C_{SE}, C_{SF}	Accompanying concentration as defined in Eq. (10a) (−)
d_e	The hydraulic diameter of the shell using Eq. (2) (m)
d_i	The inner diameter of the hollow fiber using Eq. (3) (m)
D_A, D_B, D_E, D_F	The diffusion coefficient of A, B, C, and F, respectively (m^2/s)
D_{AG}	The diffusion coefficient in the gas phase using Eq. (3) (m^2/s)
D_L	The diffusion coefficient in the liquid phase using Eq. (2) (m^2/s)
D_M	The diffusion coefficient in the membrane using Eq. (4) (m^2/s)
D_{CA}, D_{CB}, D_{CE}, D_{CF}	Diffusion rates of A, B, E, and F, as defined in Eq. (10b) (−)
I_r	The radial incurrent flux in differential cell [$mol/(m^2\,s)$]
I_Z	The axial incurrent flux in differential cell [$mol/(m^2\,s)$]
K_G	The overall reaction rates coefficient based on gas phase (m/s)
k_1, k_{-1}	The forward and reverse rate of constant for reaction (6) [$dm^3/(mol\,s)$]
k_2, k_{-2}	The forward and reverse rate of constant for reaction (7) [$dm^3/(mol\,s)$]
L	The axial length (m)
m	The equilibrium constant between the gas and liquid (−)
O_r, O_Z	The radial and axial excurrent flux in the differential cell [$mol/(m^2\,s)$]

r_m	The liquid boundary layer thickness (m)
r'	The dimensionless thickness (m)
R_A, R_B, R_E, R_F	The general rates of A, B, E, and F, respectively (mol/m^3s)
u_z	The average velocity of flow (m/s)
V_G	The flux of the gas (m^3/s)
V_L	The flux of the liguid (m^3/s)
z	The axial coordinate (m)
Z	The dimensionless axial coordinate (−)

Greek Letters

β	The chemical enhancement factor (−)

Subscripts

G	The gas phase
i	The component A, B, E, and F
L	The liquid phase

ACKNOWLEDGMENT

This work was supported by the National Natural Science Foundation of China (No.20206002), the Beijing NOVA program (H013610250112), and the University Doctor Science Foundation of China (No. 20020010004).

REFERENCES

1. Qi, Z. and Cussler, E.L. (1985) Hollow fiber gas membrane. *AIChE. J*, 31 (9): 1548–1553.
2. Kreulen, H., Versteeg, G.F., Smolders, C.A., and van Swaaij, W.P.M. (1993) Determination of mass transfer rates in wetted and non-wetted microporous membranes. *Chem. Eng. Sci.*, 48 (11): 2093–2100.
3. Mastson, S.L., Lopez, J., and Al Quinn, J. (1983) Separation of gases with synthetic membrane. *Chem. Eng. Sci.*, 38: 503–510.
4. Qi, Z. and Cussler, E.L. (1985) Microporous hollow fibers for gas absorption. I. Mass transfer in the liquid. *J. Membr. Sci.*, 23 (2): 321–332.
5. Nii, S., Kakeuchi, H., and Takahashi, K. (1992) Removal of CO_2 by gas absorption across a polymeric membrane. *J. Chem. Eng. Jpn.*, 25 (1): 67–72.
6. Kim, Y.S. and Yang, S.M. (2000) Absorption of carbon dioxide through hollow fiber membrane using various aqueous absorbents. *Sep. Pur Tech.*, 21: 101–109.
7. Teramoto, M., Matsuyama, H., Yamashiro, T., and Okamoto, S. (1989) Separation of ethylene from ethane by a flowing liquid membrane using silver nitrate as a carrier. *J. Membr. Sci.*, 45 (1): 115–123.

8. Shelekhin, A.B. and Beckman, I.N. (1992) Gas separation processes in membrane absorber. *J. Membr. Sci.*, 73 (1): 73–83.
9. Kreulen, H., Smolders, C.A., Versteeg, G.F., and van Swaaij, W.P.M. (1993) A specific application: mass transfer in highly viscous liquids. *J. Membr. Sci.*, 78 (2): 197–216.
10. Calabrò, V. (2002) A theoretical analysis of transport phenomena in a hollow fiber membrane bioreactor with immobilized biocatalyst. *J. Membr. Sci.*, 206 (1–2): 217–241.
11. Lee, Y., Noble, R.D., Yeom, B.-Y., Park, Y.-I., and Lee, K.-H. (2001) Analysis of CO2 removal by hollow fiber membrane contactors. *J. Membr. Sci.*, 194 (1): 57–67.
12. Yang, M.C. and Cussler, E.L. (1986) Designing hollow-fiber contactors. *AIChE J.*, 32 (11): 1910–1916.
13. Dahuron, L. and Cussler, E.L. (1988) Protein extractions with hollow fibers. *AIChE J.*, 34 (1): 130–136.
14. Leon Lapidus, L. and Pinder, G.F. (1999) *Numerical Solution of Partial Differential Equations in Science and Engineering*; Wiley-Interscience: Canada.
15. Shuzheng, Z. and Chengyue, L. (1987) Application of perpendicular position method to chemical engineering (I). *Chemical Engineering of China*, 2: 47–51.
16. Shuzheng, Z. and Chengyue, L. (1987) Application of perpendicular position method to chemical engineering (II). *Chemical Engineering of China*, 3: 43–49.
17. Jankowski, Dorothg, A. (1986) *Chemical Engineering Data Sources*; American Insitiute of Chemical Engineers.
18. Dankwerts, P.V. and Sharma, M.M. (1966) The absorption of carbon dioxide into solutions of alkalis and amines (with some notes on hydrogen sulfide and carbonyl sulfide). *Chem. Eng.*, October: 244–256.
19. Huss, A., Jr. and Ecbert, C.A. (1977) Equilibria and ion activities in aqueous sulfur dioxide solutions. *J. Phys. Chem.*, 81: 2268–2270.
20. Xu, G.-W., Zhang, C.-F., Qin, S.-J., Gao, W.-H., and Liu, H.-B. (1998) Gas-liquid equilibrium in CO2-MDEA-H_2O system and the effect of piperazine on It. *Ind. Eng. Chem. Res.*, 37: 1473–1477.
21. Zhang, C.F. (1985) *Gas Liquid Reaction and Reactor*; Chemical Industry Press of China: Beijing.
22. Brutsaert, W. and Jirka, G.H. (1984) *Gas Transfer at Water Surface*; D. Reicel Publishing Company: Boston.